Published in final edited form as:
Pharmacol Res. 2011 April ; 63(4): 341–351. doi:10.1016/j.phrs.2010.12.002.

The Characterization of Microtubule-Stabilizing Drugs as Possible Therapeutic Agents for Alzheimer's Disease and Related Tauopathies

Kurt R. Brunden[a], **Yuemang Yao**[a], **Justin S. Potuzak**[b], **Nuria Ibarz Ferrer**[a], **Carlo Ballatore**[a,b], **Michael J. James**[a], **Anne-Marie L. Hogan**[b], **John Q. Trojanowski**[a], **Amos B. Smith III**[b], and **Virginia M-Y. Lee**[a]

[a] Center for Neurodegenerative Disease Research and Institute on Aging, Department of Pathology and Laboratory Medicine, School of Medicine, University of Pennsylvania, Philadelphia, PA 19104

[b] Department of Chemistry, School of Arts and Sciences, University of Pennsylvania, Philadelphia, PA 19104

Abstract

Tau, a protein that is enriched in neurons of the central nervous system (CNS)1, is thought to play a critical role in the stabilization of microtubules (MTs). Several neurodegenerative disorders referred to as tauopathies, including Alzheimer's disease and certain types of frontotemporal lobar degeneration, are characterized by the intracellular accumulation of hyperphosphorylated tau fibrils. Tau deposition into insoluble aggregates is believed to result in a loss of tau function that leads to MT destabilization, and this could cause neurodegeneration as intact MTs are required for axonal transport and normal neuron function. This tau loss-of-function hypothesis has been validated in a tau transgenic mouse model with spinal cord tau inclusions, where the MT-stabilizing agent, paclitaxel, increased spinal nerve MT density and improved motor function after drug absorption at neuromuscular junctions. Unfortunately, paclitaxel is a P-glycoprotein substrate and has poor blood-brain barrier permeability, making it unsuitable for the treatment of human tauopathies. We therefore examined several MT-stabilizing compounds from the taxane and epothilone natural product families to assess their membrane permeability and to determine whether they act as substrates or inhibitors of P-glycoprotein. Moreover, we compared brain and plasma levels of the compounds after administration to mice. Finally, we assessed whether brain-penetrant compounds could stabilize mouse CNS MTs. We found that several epothilones have significantly greater brain penetration than the taxanes. Furthermore, certain epothilones cause an increase in CNS MT stabilization, with epothilone D demonstrating a favorable pharmacokinetic and pharmacodynamic profile which suggests this agent merits further study as a potential tauopathy drug candidate.

[1]Abbreviations: AD, Alzheimer's disease; BBB, blood-brain barrier; B/P, brain-to-plasma; CNS, central nervous system; FTDP-17, frontotemporal dementia with Parkinsonism linked to chromosome 17; MDCK-MDR, Madin-Darby canine kidney cells expressing MDR1; MT, microtubule; NF, neurofilament; NGF, nerve growth factor; ON, optic nerve; Pgp, P-glycoprotein.

Corresponding Author: Kurt R. Brunden, Ph.D., Director of Drug Discovery, Center for Neurodegenerative Disease Research, Department of Pathology and Laboratory Medicine, University of Pennsylvania, 3600 Spruce St., Maloney 3rd Floor, Philadelphia, PA 19104, Phone: 1-215-615-5262, Fax: 1-215-349-5909 kbrunden@upenn.edu.

Keywords

Alzheimer's disease; microtubules; tauopathies; therapeutic

1. Introduction

The MT-associated protein tau forms filamentous inclusions within neurons in several CNS disorders, including Alzheimer's disease (AD)[1] and certain frontotemporal dementias [1–3]. Collectively, these diseases are referred to as tauopathies, and alterations in normal tau structure and/or function likely play a causative role in the neuropathology of these various conditions. Indeed, tau gene (*MAPT*) mutations cause frontotemporal dementia with Parkinsonism linked to chromosome 17 (FTDP-17) [4;5], and dementia ratings in AD are correlated with the extent of tau brain deposits [6;7].

Tau is highly expressed in neurons, where it plays a critical role in MT stabilization [8;9] and axonal transport. The tau hyperphosphorylation that occurs in all tauopathies [10;11] results in reduced tau binding to MTs and a decreased ability to promote MT assembly [12–16]. Moreover, tau phosphorylation has been reported to enhance its propensity to fibrillize [17;18] and this could cause destabilization of MTs due to the depletion of free tau.

The concept that neuropathology can result from tau loss-of-function is supported by studies that showed MT abnormalities and axonal transport deficits in motor axons of transgenic (Tg) mice that over-express human tau [19]. Importantly, impaired tau function was compensated for in these mice by treatment with the MT-stabilizing agent paclitaxel, as drug absorption by motor neurons at peripheral neuromuscular junctions resulted in increased MT density and marked improvement in motor function [20]. These data suggest that MT-stabilizing drugs that are utilized in oncology may be potential therapeutics for AD and other tauopathies. However, paclitaxel and most related taxanes are thought to have poor blood-brain barrier (BBB) permeability and are thus likely unsuitable for the treatment of human tauopathies, where pathology is predominantly in the brain. Accordingly, compensation for tau loss-of-function in tauopathies will require brain-penetrant MT-stabilizing agents.

The relative inability of paclitaxel and analogues to enter the brain is believed to be due in part to these compounds acting as substrates for the P-glycoprotein (Pgp) transporter that resides in endothelial cells that form the BBB [21;22]. Taxane derivatives have been prepared that retain anti-mitotic activity in Pgp-expressing cells [23–25], but this activity appeared to result from the compounds inhibiting Pgp function [26;27]. Similarly, other taxanes such as TXD258 [28] and RPR-109881A [29] have been reported to accumulate in the brain, although the former is a modest Pgp substrate that may saturate the transporter at high blood drug levels [28]. Because Pgp plays an important role in shielding the brain from undesirable xenobiotics, inhibitors of Pgp or substrates that impede Pgp function could be detrimental as therapeutics for chronic disorders like AD and related tauopathies. Accordingly, we [30] and others [31] have reported on the synthesis of novel taxane analogs that are neither Pgp substrates or inhibitors. Here we report on the further characterization of such molecules, as well as examples from the epothilone class of MT-stabilizing agents. The compounds were evaluated in cell-based assays to assess whether they interact with Pgp and to gauge their membrane permeability. Moreover, because there is little published

[1]Abbreviations: AD, Alzheimer's disease; BBB, blood-brain barrier; B/P, brain-to-plasma; CNS, central nervous system; FTDP-17, frontotemporal dementia with Parkinsonism linked to chromosome 17; MDCK-MDR, Madin-Darby canine kidney cells expressing MDR1; MT, microtubule; NF, neurofilament; NGF, nerve growth factor; ON, optic nerve; Pgp, P-glycoprotein.

information on the brain penetration of existing MT-stabilizing agents *in vivo*, we compared the brain and plasma levels of these compounds in mice after systemic administration. Finally, we determined whether these molecules can affect CNS MTs in mice, utilizing a marker of MT stabilization (i.e., tubulin acetylation). We find that members of the epothilone series of MT-stabilizing compounds have much greater BBB penetration than the tested taxanes. Moreover, certain of the epothilones cause a significant increase in MT stabilization within the CNS. Thus, we have identified candidate MT-stabilizing compounds that are suitable for testing in Tg mouse models of tauopathy, and certain of these may hold promise as possible therapeutic agents for AD and related tauopathies.

2. Materials and Methods

2.1 Reagents

Tissue culture medium and penicillin/streptomycin were purchased from Mediatech (Manassas, VA). Fetal bovine serum was from Hyclone/Thermo Scientific (Waltham, MA), and horse serum was obtained from SAFC Biosciences/Sigma-Aldrich (St. Louis, MO). Mouse nerve growth factor (NGF) was purchased from Collaborative Biomedical Products (Bedford, MA). All protease inhibitors were from Sigma-Aldrich. Ixabepilone was obtained from the University of Pennsylvania Hospital pharmacy. All HPLC solvents were purchased from Fisher Scientific (Pittsburgh, PA). Acetyl-tubulin antibody (6-11B-1) was from Sigma-Aldrich, 12G10 α-tubulin antibody was purified from culture supernatant of hybridoma cells obtained from the Developmental Studies Hybridoma Bank at the University of Iowa, and RMO189 neurofilament (NF) medium chain antibody was developed in-house [32]. BlockAce was obtained from AbD Serotec (Oxford, UK). HRP-conjugated anti-mouse IgG was from Jackson Immunoresearch (West Grove, PA). Horse radish peroxidase labeling of antibodies was with a Peroxidase Labeling Kit (Roche Applied Science, Indianapolis, IN). TMB-peroxidase substrate was obtained from KPL (Gaithersburg, MD). Protein A/G plus-agarose beads were purchased from Santa Cruz Biotechnology (Santa Cruz, CA). BCA protein determination reagent was from Thermo Scientific.

2.2 Synthesis of Epothilones

Epothilone D (CNDR-66) and its closely related congeners (CNDR-85–87), as well as 12,13-desoxy-epothilone F (CNDR-89) and its 9,10-dehydro synthetic precursor (CNDR-88), were prepared as previously described by Danishefsky and coworkers [33–35].

2.3 MDCK-MDR Assays

Bi-directional permeability studies employing Madin-Darby canine kidney cells transfected with human MDR1 (MDCK-MDR) were conducted by Absorption Systems, Inc. (Exton, PA) to determine the membrane permeability and Pgp transport liability of test compounds. Briefly, MDCK-MDR monolayers were grown to confluence on collagen-coated, microporous, polycarbonate membranes in 12-well plates. The permeability assay buffer was Hanks Balanced Salt Solution containing 10 mM HEPES and 15 mM glucose at a pH of 7.4. Test compounds were added to the assay buffer at a concentration of 5 μM. For Pgp inhibition studies, 10 μM digoxin was incubated in the absence or presence of 5 μM test compound. Cell monolayers were dosed on the apical (A) or basolateral (B) compartment and incubated at 37°C with 5% CO2 in a humidified incubator. After 1 and 2 hours, aliquots were taken from the receiver chambers and replaced with fresh assay buffer. Samples were taken from the donor chamber after 2 hours. Each determination was performed in duplicate. The lucifer yellow flux was also measured for each monolayer to ensure no damage was inflicted to the cell monolayers during the measurement period. Compound concentrations in the samples were determined by LC-MS/MS using electrospray ionization. The apparent

permeability coefficient, Papp, in both the A-B and B-A directions, as well as percent recovery and efflux ratio, were calculated as follows:

$$\text{Papp} = (d\text{Cr}/d\text{t}) \times \text{Vr}/(\text{A} \times \text{CN})$$
$$\text{Percent Recovery} = 100 \times ((\text{Vr} \times \text{Crfinal}) + (\text{Vd} \times \text{Cdfinal}))/(\text{Vd} \times \text{CN})$$
$$\text{Efflux Ratio} = \text{P}_{\text{appB-A}}/\text{P}_{\text{appA-B}}$$

where,

*d*Cr /*d*t is the slope of the cumulative concentration in the receiver compartment versus time in μM/s; Vr is the volume of the receiver compartment in cm^3; Vd is the volume of the donor compartment in cm^3; A is the area of the cell monolayer (1.13 cm^2 for 12-well plates); CN is the nominal concentration of the dosing solution in μM; Crfinal is the cumulative receiver concentration in μM at the end of the incubation period and; Cdfinal is the concentration of the donor in μM at the end of the incubation period.

2.4 Compound Treatments

All compounds were dissolved in 100% DMSO. For the MDCK-MDR and PC12 cell culture studies, compounds were diluted at least 1:1000 into culture medium before addition to cells. All mice (B6C3F1) received test compounds dissolved in DMSO via intraperitoneal (i.p.) administration of volumes of ~40 μl, with volume adjusted to body weight to ensure the proper dosage. Young male B6C3F1 mice (2–3 months of age) were utilized in all studies, with the number of mice per treatment group indicated in the figure legends.

2.5 PC12 Cell Culture Model

PC12 cells were grown essentially as described [36]. Briefly, cells were maintained in RPMI medium containing 5% fetal bovine serum, 10% horse serum, 50 units/ml penicillin, and 50 μg/ml streptomycin. For testing of drugs, cells were dissociated with trypsin/EDTA and replated at 4×10^5 cells/well into 6-well plates. After ~6 hours of incubation, the medium was aspirated and new RPMI medium (2 ml) was added that contained NGF (200 ng/ml) and test compound. Following 24 hours of incubation, cells were washed with 1 ml of ice-cold phosphate-buffered saline, pH 7.4 (PBS), followed by 0.15 ml/well of ice-cold RIPA buffer (0.5% sodium deoxycholate, 0.1% SDS, 1% NP-40, 5 mM EDTA, pH 8.0) containing protease inhibitor mix (1 μg/ml each of pepstatin, leupeptin, TLCK, TPCK and trypsin inhibitor), 1 mM PMSF and 1 μM trichostatin A (buffer designated RIPA-INH). The cell-buffer mixture was scraped from the wells and transferred to 1.5 ml microfuge tubes. After centrifugation for 30 minutes at 15,000g, supernatants were collected and protein concentrations were determined using a BCA assay.

2.6 Optic Nerve and Brain Homogenate Preparation for ELISA

Optic nerve and whole brain hemispheres obtained from mice euthanized using protocols approved by the University of Pennsylvania Institutional Animal Care and Use Committee were homogenized and then briefly sonicated with a handheld sonicator in 1:5 w/v RIPA-INH buffer. The homogenates were centrifuged at 100,000g for 30 minutes at 4°C, and the supernatants were collected. The supernatant samples were diluted 1:15 in RIP-INH before protein determination with a BCA assay.

2.7 Acetyl-Tubulin Immunoblotting

Aliquots of PC12 cell homogenates (2.5 μg of total homogenate protein) were analyzed by SDS-PAGE (10% gel) with subsequent immunoblotting using acetyl-tubulin antibody

(1:3000 v/v) or RMO189 NF-M antibody (1:2000 v/v), followed by HRP-conjugated anti-mouse IgG (1:2000 v/v). The blot was incubated with Western Lightning–ECL (Perkin Elmer Life Sciences) for 1 minute, followed by densitometric analysis using a Fujifilm LAS-3000 densitometer.

2.8 Acetyl-Tubulin ELISA

384-well plates were coated with 12G10 α-tubulin antibody (10 μg/ml) in 30 μl of cold 0.1 M bicarbonate buffer. After overnight incubation at 4°C, the plates were washed with cold PBS, followed by the addition of Block-Ace solution and overnight incubation at 4°C. The blocking solution was removed and 10 μl of EC buffer (0.02 M sodium phosphate, pH 7.0, 2 mM EDTA, 0.4 M NaCl, 0.2% bovine serum albumin, 0.05% CHAPS, 0.4% BlockAce and 0.05% NaN_3) was added to each well. Cell culture or tissue homogenates were diluted in EC buffer (typically three-fold dilutions from 60 ng/μl to 2.2 ng/μl) and 30 μl of each were added to wells in duplicate and plates were subsequently sealed. After overnight incubation at 4°C, the plates were aspirated and washed with cold PBS containing 0.05% Tween-20 and 0.05% thimerisol (PBS-Tween buffer), followed by addition of 30 μl/well of HRP-conjugated acetyl-tubulin antibody labeled (prepared with a Peroxidase Labeling Kit following the manufacturer's instructions) that was diluted 1:6000 in C buffer (0.02 M sodium phosphate, pH 7.0, 2 mM EDTA, 0.4 M NaCl, 1% bovine serum albumin and 0.05% thimerisol). The plates were incubated at room temperature for 4 hours on a platform rocker, followed by washing with cold PBS-Tween buffer. Peroxidase substrate solution (30 μl) was added and the reaction was quenched after 5–10 minutes by addition of 30 μl of 10% phosphoric acid. Plates were read on a SpectraMax M5 plate reader at 450 nm. Because an acetyl-tubulin standard is not available, all data were normalized to a control treatment condition (e.g., no compound addition). Typically, control acetyl-tubulin OD readings were plotted against the log of input homogenate sample to generate a linear curve (see Supplemental Figure 1). OD readings obtained from homogenates of experimental samples were then fit to the control input curve to obtain a calculated "control-normalized" protein equivalent amount (Supplemental Figure 1). These values can then be divided by the corresponding value obtained from the standard curve for the vehicle-treated control samples to yield the relative change in acetyl-tubulin levels. At least two different experimental homogenate protein input amounts in duplicate were used to obtain the "control-normalized" protein equivalent values for each experimental treatment.

2.9 Acetyl-Tubulin Immunoprecipitation

Mouse brain and optic nerve homogenates were prepared as described in section 2.6. An aliquot of each (input fraction) in RIPA-INH buffer (20 μg total protein; volumes of ~20–40 μl) was treated with 10 μl of undiluted acetyl-tubulin antibody and incubated overnight at 4°C with mixing. Protein A/G-plus agarose beads (50 μl) were subsequently added to the mixture, followed by an additional 2 hour incubation at 4°C with mixing. The immunoprecipitation mix was centrifuged in a microfuge at 1400g for 2 minutes and the supernatant was removed (supernatant fraction) and the volume noted. The agarose bead pellet was washed three times with RIPA-INH buffer and bound material was then removed by the addition of 0.1 ml of SDS-PAGE loading buffer followed by centrifugation, with the supernatant removed (pellet fraction) and the volume noted. Aliquots corresponding to 20% of the total input, supernatant and pellet fraction volumes were analyzed by SDS-PAGE (10% gel) and immunoblotted with either acetyl-tubulin antibody (1:3000 v/v) or 12G10 α-tubulin antibody (1:2000 v/v), followed by HRP-conjugated anti-mouse IgG (1:2000 v/v). The blot was subsequently incubated with Western Lightning–ECL (Perkin Elmer Life Sciences) for 1 minute, and the blot was analyzed by densitometry using a Fujifilm LAS-3000 densitometer

2.10 Determination of Plasma and Brain Compound Concentrations

Mouse brains were homogenized in 10 mM ammonium acetate, pH 5.7 (1:2; w/v) using a handheld sonic homogenizer. Mouse plasma was obtained from blood that was collected into a 1.5 ml tube containing 0.5M EDTA solution and which was centrifuged for 10 minutes at 4500g at 4°C. Aliquots (50 μl) of brain homogenates or plasma were mixed with 0.2 ml of acetonitrile, centrifuged at 15,000g, and the resulting supernatant was used for subsequent LC-MS/MS analysis. The LC-MS/MS system was comprised of an Aquity UPLC and a TQ MS that was controlled using MassLynx software (Waters Corporation, Milford, MA, USA). Compounds were detected using multiple reaction monitoring (MRM) of their specific collision-induced ion transitions. Samples were separated on an Aquity BEH C18 column (1.7 μm, 2.1 × 50 mm) at 35 C. Operation was in positive electrospray ionization mode, with mobile phase A of 0.1% (v/v) formic acid, and B of either acetonitrile or methanol with 0.1% (v/v) formic acid. Injections of 5 μl were separated at a flow rate of 0.6 mL/min using a gradient from 5% to 95% B over two minutes, followed by wash and re-equilibration steps. The MS was operated with a desolvation temperature of 450 C and a source temperature of 150 C. Desolvation and source nitrogen gas flows were 900 L/hr and 50 L/hr, respectively. Source and MS/MS voltages were optimized for each compound using the MassLynx auto tune utility. To account for possible matrix effects on analytes, standard curves were generated for each compound from brain homogenate and plasma samples that had compound added at 4, 40, 400 and 4000 ng/mL. The standard curve samples were extracted and analyzed in an identical fashion as the corresponding tissue-derived samples, and peak areas were plotted against concentration and a 1/x weighted linear regression curve was used to obtain estimated concentrations of the tissue-derived samples using the average peak area from triplicate injections. In all cases, the tissue-derived sample peak areas fell within the linear portion of standard curves that were prepared and analyzed concurrently with the samples.

2.11 Determination of Drug Plasma and Brain Non-Specific Binding

The unbound fractions of drug in mouse plasma and brain were determined using a rapid equilibrium dialysis (RED) plate (Pierce Biotechnology, Rockford, IL). Test compounds were mixed at a concentration of 1 μM with mouse plasma or brain homogenate that was diluted 3-fold with 100 mM sodium phosphate, pH 7.4. Triplicate 100 μl aliquots were placed in sample chambers and dialyzed against 300 μl of 100 mM sodium phosphate, pH 7.4, for five hours at 37 C with shaking at 100 rpm. In order to achieve identical sample composition between buffer and non-buffer samples, a 20 μL aliquot was removed from the sample chamber and mixed with an equal volume of dialysis buffer. A 20 μl aliquot was removed from the buffer chamber was mixed with an equal volume of plasma or brain homogenate. Compounds were extracted with 120 μl acetonitrile, vortexed and centrifuged at 15,000g for 15 minutes. Supernatants were analyzed by HPLC-MS/MS. Unbound fraction was calculated using the ratio of MS/MS ion-specific peak areas from the buffer and sample chambers. Brain unbound fraction was calculated using the following equation, adjusting for tissue dilution (D).

$$\text{Undiluted } f_u = \frac{1/D}{((1/f_{u,\text{measured}}) - 1) + 1/D}$$

2.12 Statistical Methods

Compound and vehicle treatment effects were compared by one-way ANOVA with Dunnett's post-hoc analysis using GraphPad Prism software. The number of replicates in each study is indicated in the figure legends.

3. Results

3.1 Evaluation of Selected Taxanes and Epothilones for Pgp transport and BBB Penetration

The inability of paclitaxel to enter the CNS readily is believed to be due in part to efflux by Pgp. Paclitaxel analogs that are not Pgp substrates or inhibitors have been reported both by our laboratory [30] and others [24;31]. However, even these improved taxanes generally have a relatively low apical-to-basolateral (A-B) permeability coefficient values (i.e., $<1 \times 10^{-6}$ cm/s) in a MDCK-MDR cell bi-directional permeability assay [30;37]. This reflects poor diffusion across the MDCK cell membranes and suggests poor BBB penetration [37], although the value of these cells in predicting brain penetration does not appear to be as good as, for example, brain capillary endothelial cells [38]. It has previously been reported that CNDR-3 and CNDR-29 (Figure 1) are not Pgp substrates as evidenced by (B-A)/(A-B) efflux ratios near unity, yet both have A-B permeability coefficients of $<0.1 \times 10^{-6}$ cm/s [30]. To confirm that CNDR-3 or CNDR-29 have poor BBB permeability, as suggested by the MDCK-MDR studies, we assessed plasma and brain concentrations of these agents, as well as paclitaxel, two hours after intraperitoneal (i.p.) administration of a 5 mg/kg dose to mice. Although readily measurable amounts of CNDR-3 and CNDR-29 were observed in the plasma, neither of these compounds could be detected in the brain (Table 1). Paclitaxel was present in the brain, but the relative concentration was only 7% of that found in the plasma. Most CNS-active drugs have brain-to-plasma (B/P) ratios >0.3 [39], although there can be exceptions. For example, brain-penetrant drugs with a low unbound plasma fraction due to high plasma protein binding could show very low B/P ratios if the unbound fraction in brain is much greater than in the plasma (i.e., total drug B/P = [(free drug in brain) X (fraction unbound in plasma)]/[(free drug in plasma) X (fraction unbound in brain)]) [40]. However, we have determined by standard equilibrium dialysis methods [41] that the unbound fractions of paclitaxel in mouse plasma and brain are not dramatically different (3% and 1%, respectively). Thus, the low B/P value of pacliltaxel is due to poor partitioning across the BBB, and it and the other tested taxanes appear to have insufficient brain penetration to be of potential utility for tauopathies.

In an attempt to identify MT-stabilizing compounds that might have greater BBB penetration, we synthesized or purchased a number of examples from the epothilone family (Figure 1) of anti-cancer compounds [42;43]. To simplify further discussion, we have assigned a compound identification number to each of the tested epothilones, as summarized in Figure 1. While structurally distinct from the taxanes, the epothilones appear to act by a similar mechanism and share a common MT binding site with paclitaxel [44]. Moreover, epothilone D (CNDR-66) has been reported to improve outcomes in a mouse schizophrenia model [45] and epothilone B has been reported to enter the brain [46]. Thus, these molecules and perhaps other related analogues might be expected to penetrate the BBB.

An evaluation of various epothilones in the MDCK-MDR permeability assay revealed that CNDR-86, CNDR-88 and CNDR-89 had efflux ratios >10 (Table 2), suggesting that they are Pgp substrates. However, CNDR-66 had an efflux ratio that was near unity, indicating that it is likely not transported by Pgp. Moreover, CNDR-85 and CNDR-87 had efflux ratios <10, which would suggest that they are relatively modest substrates for Pgp. We further examined the potential interactions of the epothilones with Pgp by evaluating their ability to act as inhibitors of the transporter. As summarized in Table 3, although CNDR-66 appeared to be a poor Pgp substrate, it was a potent inhibitor of Pgp transport as evidenced by its ability to significantly decrease the B-A permeability of the Pgp substrate, digoxin. Both CNDR-85 and CNDR-87 also inhibited digoxin transport, although to a lesser extent than CNDR-66 (Table 3). Although each of the epothilones appeared to interact with Pgp, either as a substrate or inhibitor, it was noteworthy that all but CNDR-88 had A-B permeability

coefficients that were $\gg 1 \times 10^{-6}$ cm/s, with CNDR-66 and CNDR-87 having the largest values. This implies that members of the epothilone series might readily cross membrane bilayers by passive diffusion and thus gain access to the brain. This was confirmed in studies in which drug levels in the plasma and brain were assessed 2 hours and 24 hours after dosing at 5 mg/kg and 10 mg/kg, respectively (Table 1). Each of the epothilones had high compound levels in the brain at two hours, and all but CNDR-90 (ixabepilone) had total drug B/P ratios that exceeded unity at this time. Importantly, significant amounts of all the epothilones persisted in the brains 24 hours after a single administration although, with the exception of CNDR-90, the plasma levels of the compounds were low or undetectable at this time. Thus, all of the epothilones, including those that appear to be Pgp substrates, readily cross the BBB and gain access to the brain. However, the greater B/P ratios observed at 24 hours after dosing compared to two hours indicates that the compounds are retained in the brain. This was confirmed by a full pharmacokinetic analysis of CNDR-66, where the brain levels of the drug persisted with an elimination half-life which far exceeded that observed in the plasma (data not shown). This prolonged brain stability would suggest that the compounds are not in full equilibrium with the blood after entering the brain, being retained via non-specific protein /lipid interactions and/or specific binding to MTs.

3.2 Evaluation of CNS MT Stabilization by Epothilones

To determine whether these BBB-permeable epothilones can elicit MT stabilization within the CNS, we employed acetylated-tubulin as a biomarker as it is known that α-tubulin within stable MTs becomes acetylated at lysine-40, and conversely, that non-polymerized α-tubulin is rapidly deacetylated [47;48]. To facilitate the measurement of acetyl-tubulin within cell or tissue homogenates, a specific acetyl-tubulin sandwich ELISA was developed. To validate the ELISA, PC12 cells were treated with increasing concentrations of CNDR-66 for 24 hours, followed by a comparison of the acetyl-tubulin levels in cell homogenates as determined by both immunoblotting and ELISA. Whereas control PC12 cells had very little detectable acetyl-tubulin upon immunoblotting (Figure 2a), treatment with CNDR-66 resulted in a significant concentration-dependent increase in the amount of acetyl-tubulin that was quantified by densitometric analysis of immunoblots (Figure 2b). Determination of acetyl-tubulin levels with the ELISA yielded increases that were comparable to those observed by immunoblotting (Figure 2c). A similar concentration-dependent increase of acetyl-tubulin can also be obtained when PC12 cells are treated with a taxane MT-stabilizing drug (not shown). Thus, the ELISA provides a convenient method to assess levels of acetyl-tubulin from homogenate samples.

The epothilones were subsequently administered at doses of 1, 3 and 10 mg/kg to normal mice, followed by ELISA measurement of acetyl-tubulin in brain homogenates prepared 16 hours after dosing. Although all of the compounds achieved appreciable brain concentrations 16 hours after administration of 10 mg/kg (Figure 3c), little change was observed in brain acetyl-tubulin levels relative to vehicle-treated animals (Figure 3a). CNDR-89 caused an increase of acetyl-tubulin relative to vehicle at 3 mg/kg, but this result is likely a statistical anomaly since no effect was observed at 10 mg/kg even though the brain levels of the compound were correspondingly greater at this dose than at 3 mg/kg. The inability to demonstrate significant increases in brain acetyl-tubulin after overnight treatment with the epothilones might reflect the fact that the vast majority of α-tubulin within normal brain neurons is already incorporated into MTs and thus acetylated. In fact, a recent study demonstrated that immunoprecipitation of acetyl-tubulin from mouse brain homogenates resulted in the capture of essentially all of the α-tubulin, indicating that there was virtually no α-tubulin that was deacetylated [49]. This contrasted with peripheral tissues, where a large percentage of the α-tubulin appeared to be deacylated [49]. We also found that the vast majority of total α-tubulin within normal mouse brain was

immunoprecipitated with acetyl-tubulin antibody (Figure 4), confirming that there is very little deacetylated α-tubulin.

Although increases of tubulin acetylation were not observed in the brains of mice 16 hours after administration of the epothilones, we also examined the optic nerve (ON), which lies entirely within the CNS and is enriched in large caliber retinal ganglion cell axons which contain abundant MTs. We reasoned that this tissue might prove to be more sensitive to changes in MT markers because immunoprecipitation of ON homogenates with acetyl-tubulin antibody revealed a greater fraction of deacetylated α-tubulin in ON than in brain (Figure 4), suggesting that the ON has a larger pool of free α-tubulin that could be incorporated into MTs upon treatment with a MT-stabilizing drug. As shown in Figure 3b, increases of acetyl-tubulin of up to ~50% were observed in the ON 16 hours after treatment with four of the tested epothilones. The magnitude of the acetyl-tubulin increase caused by the epothilones is in approximate agreement with the fraction of deacetylated α-tubulin within the ON (Figure 4), suggesting that the active epothilones facilitated conversion of the non-polymerized α-tubulin into polymerized MTs. CNDR-66 and CNDR-87 caused the most profound effect, with an elevation of acetyl-tubulin at all doses. CNDR-85 and CNDR-89 treatment only resulted in an increase of the stabilized MT biomarker at 10 mg/kg, whereas neither CNDR-86 nor CNDR-88 elicited a change at any dose even though these compounds crossed the BBB, as evidenced by appreciable brain levels 16 hours after dosing (Figure 3a).

There was a general correlation between compound ON activity and the efflux ratio determined in the MDCK-MDR assay (Table 2), and it is possible that the lack of appreciable Pgp transport of CNDR-66 and CNDR-87 resulted in higher free (unbound) drug levels than for the epothilones that are readily transported by Pgp. Thus, while compound BBB penetration is a necessity for CNS MT stabilization, brain total drug levels may not be entirely predictive of MT stabilization in the ON and the different activities observed among the tested epothilones could reflect differences in brain free drug concentrations. It is also possible that the measured brain concentrations of compounds do not entirely reflect drug levels in the ON. Unfortunately, we could not determine drug concentrations in the ON as there was insufficient tissue mass to allow accurate LC-MS/MS determinations.

3.3 CNDR-66 (Epothilone D) Causes a Delayed Increase in Brain Acetyl-Tubulin Levels

The low levels of deacetylated α-tubulin in normal mouse brain suggested that there was very little free α-tubulin that could be further recruited to MTs. Nonetheless, we assessed whether changes in tubulin acetylation might occur at times later than 16 hours after treatment with CNDR-66. Interestingly, a single administration of 3 mg/kg resulted in increased acetyl-tubulin levels that were observable 6 and 10 days after a single drug dosing (Figure 5a). This observation suggested that CNDR-66 persisted in the brain for an extended period and caused a slow increase in α-tubulin acetylation. Quantification of CNDR-66 in brain tissue confirmed that there were detectable levels of the drug 7 and 10 days after dosing (8.3 +/− 1.0 ng/g and 1.8 +/− 0.1 ng/g, respectively).

To gain further understanding of the pharmacodynamic (PD) effects of a single administration of CNDR-66, we compared brain acetyl-tubulin levels 7 and 14 days after a 3 mg/kg dose. As shown in Figure 5b, we observed an increase of acetyl-tubulin at 7 days that diminished to a statistically insignificant change at 14 days after dosing. An exploration of the dose-dependency of the CNDR-66 effect on brain MTs revealed that a 1 mg/kg dose also resulted in a significant increase of brain acetyl-tubulin at 7 days (Figure 6a), although this effect was somewhat lower than that observed with 3 mg/kg. Acetyl-tubulin level was not further increased by dosing at 6 mg/kg.

The ability to elicit a desired biological response with CNDR-66 in the brains and ON of mice at doses as low as 1 mg/kg is noteworthy as this is ~1/30 of the human equivalent dose (based on mg/m^2) was used in the testing of this compound (epothilone D) in cancer patients [50]. Overnight treatment with 1 mg/kg of CNDR-87 also led to a significant increase of ON acetyl-tubulin (Figure 3b), and we thus tested whether this epothilone could elicit increased tubulin acetylation in the brain one week after dosing. Interestingly, no changes in brain acetyl-tubulin levels were observed 7 days after dosing with 3 or 6 mg/kg of CNDR-87 (Figure 6b). However, an evaluation of brain drug levels revealed that there were undetectable amounts of CNDR-87 at this time, suggesting that CNDR-87 does not persist in the brain as long as CNDR-66.

4. Discussion

Although tau-mediated MT dysfunction in a Tg mouse model could be overcome by treatment with the MT-stabilizing drug paclitaxel [20], these results cannot be translated directly to human tauopathies because the affected motor neurons in these Tg animals absorbed paclitaxel at neuromuscular junctions. In AD and other tauopathies, tau pathology is found predominantly in the brain and the poor BBB permeability of paclitaxel indicates that this drug would likely not be efficacious. Accordingly, experiments were conducted to identify MT-stabilizing drugs that readily penetrate the brain and which might hold promise for the treatment of human tauopathies.

Neither paclitaxel, nor two paclitaxel analogues that did not appear to be appreciably transported by Pgp, readily crossed the BBB after administration to mice. In contrast, all tested examples from the epothilone family of MT-stabilizing agents, including those that appeared to be Pgp substrates, had high brain compound levels two hours after dosing. Moreover, significant quantities of all the epothilones remained in the brain 24 hours after administration, although plasma compound levels dropped appreciably. The high brain concentrations of compound may reflect high non-specific binding in the brain and/or specific interaction with MTs.

Although PK analyses revealed that significant amounts of the epothilones could cross the BBB and enter the brain, it was important to establish that the desired CNS MT-stabilizing activity was elicited by these compounds. Relative CNS acetyl-tubulin levels were employed as a surrogate marker of polymerized MTs, as it has previously been demonstrated that α-tubulin within stable MTs is acetylated and that depolymerized α-tubulin is rapidly deacetylated [48]. Furthermore, acetyl-tubulin has previously been utilized as a PD marker in non-CNS tissue during evaluation of MT-stabilizing drugs in oncology trials [51]. Evaluation of brain homogenates derived from normal mice 16 hours after receiving 3 mg/kg doses of the epothilones revealed that there were no consistent changes in acetyl-tubulin even though brain drug levels of >100 nM were achieved. The absence of a significant effect in mouse brain likely reflects a scarcity of free deacetylated α-tubulin, as previously suggested [49] and confirmed by our analyses. In contrast, we demonstrated that the ON contains a greater amount of deacetylated α-tubulin and we observed a dose-dependent elevation of ON α-tubulin acetylation after treatment with a subset of the epothilones.

Although the epothilones had no effect on brain α-tubulin acetylation 16 hours after dosing, we observed a significant increase of this biomarker six days after administration of CNDR-66 at 3 mg/kg that persisted through 10 days. Measurable amounts of CNDR-66 were found in the brain at these time points, and it is possible that much of the drug was bound to MTs. Although the mechanism leading to the delayed increase in brain acetyl-tubulin is not fully understood, it may result from a gradual up-regulation of α-tubulin

synthesis that occurs in response to incorporation of free α-tubulin into MTs after drug treatment [52]. Over time, the continued incorporation of new α-tubulin into MTs could result in a measurable increase of brain acetyl-tubulin. The ability to measure a marker of stabilized MTs within days of compound administration provides a valuable pharmacodynamic readout that allows for the rapid evaluation of MT-stabilizing compounds that might have potential for the treatment of tauopathies.

Whereas CNDR-66 treatment at 1 mg/kg resulted in a significant increase of brain acetyl-tubulin 7 days after dosing, CNDR-87 at doses up to 6 mg/kg was ineffective. Although CNDR-87 was comparable to CNDR-66 in its elevation of ON acetyl-tubulin 16 hours after dosing, the absence of brain activity likely relates to its shorter residence time, as CNDR-87 was not detectable in brain tissue 7 days after administration.

5. Conclusions

Epothilone D (CNDR-66) has favorable CNS PK-PD attributes, as this compound readily crosses the BBB and upon entering the brain displays a half-life that exceeds that observed in the blood. Although having a drug retained in the brain is often undesirable, this may be a beneficial feature for the treatment of tauopathies as the MT-stabilizing drug could be eliminated from the periphery, thereby diminishing toxic action on normal dividing cells that results in side-effects such as neutropenia [53]. The prolonged brain exposure to epothilone D may also explain why a dose that is ~30-fold less than that used in human clinical testing [50] elicited a significant PD effect in the mouse brain. The observation that epothilone D appears to be a Pgp inhibitor raises a potential safety concern, as this compound could affect the ability of Pgp to protect the brain from undesirable xenobiotics. However, the long duration of action of epothilone D in the brain and the resulting infrequent dosing could minimize the amount of time that Pgp is compromised by high epothilone D levels in the blood. The studies described here have resulted in the recent testing of epothilone D in Tg mice that express mutant human tau and which develop forebrain accumulations of tau, synaptic degeneration and neuronal death [54]. Epothilone D was found to improve CNS axonal integrity, MT density and cognitive performance in these Tg mice without eliciting observable side-effects [55], suggesting that the PK-PD testing described herein provides a useful paradigm for the evaluation of MT-stabilizing agents with potential value for the treatment AD and related tauopathies. Future evaluation of epothilone D, as well as additional brain-penetrant MT-stabilizing agents, in Tg mouse models of tauopathy will provide important information on the potential benefits and relative safety profile of such drugs for the treatment of AD and related diseases.

Supplementary Material

Refer to Web version on PubMed Central for supplementary material.

Acknowledgments

We thank Drs. Hugo Geerts and Donna Huryn for helpful discussions, Dr. Edward Hyde for his assistance with assay development, and our colleagues at CNDR for their contributions to this study. This work was supported by a grant from the National Institute on Aging of the National Institutes of Health [U01 AG24904] and the Marian S. Ware Alzheimer Program.

References

1. Brunden KR, Trojanowski JQ, Lee VMY. Advances in tau-focused drug discovery for Alzheimer's disease and related tauopathies. Nat Rev Drug Discov 2009;8:783–93. [PubMed: 19794442]

2. Ballatore C, Lee VMY, Trojanowski JQ. Tau-mediated neurodegeneration in Alzheimer's disease and related disorders. Nat Rev Neurosci 2007;8:663–72. [PubMed: 17684513]

3. Lee VMY, Goedert M, Trojanowski JQ. Neurodegenerative tauopathies. Annu Rev Neurosci 2001;24:1121–59. [PubMed: 11520930]

4. Hutton M, Lendon CL, Rizzu P, Baker M, Froelich S, Houlden H, et al. Association of missense and 5 '-splice-site mutations in tau with the inherited dementia FTDP-17. Nature 1998;393:702–5. [PubMed: 9641683]

5. Hong M, Zhukareva V, Vogelsberg-Ragaglia V, Wszolek Z, Reed L, Miller BI, et al. Mutation-specific functional impairments in distinct Tau isoforms of hereditary FTDP-17. Science 1998;282:1914–7. [PubMed: 9836646]

6. Arriagada PV, Growdon JH, Hedleywhyte ET, Hyman BT. Neurofibrillary tangles but not senile plaques parallel duration and severity of Alzheimers disease. Neurology 1992;42:631–9. [PubMed: 1549228]

7. Wilcock GK, Esiri MM. Plaques, tangles and dementia - a quantitative study. J Neurol Sci 1982;56:343–56. [PubMed: 7175555]

8. Drechsel DN, Hyman AA, Cobb MH, Kirschner MW. Modulation of the dynamic instability of tubulin assembly by the microtubule-associated protein tau. Mol Biol Cell 1992;3:1141–54. [PubMed: 1421571]

9. Trinczek B, Biernat J, Baumann K, Mandelkow EM, Mandelkow E. Domains of Tau-Protein, Differential Phosphorylation, and Dynamic Instability of Microtubules. Mol Biol Cell 1995;6:1887–902. [PubMed: 8590813]

10. Avila J. Tau and tauopathies: tau phosphorylation and tau assembly. FEBS J 2006;273:23.

11. Avila J. Tau phosphorylation and aggregation in Alzheimer's disease pathology. FEBS Lett 2006;580:2922–7. [PubMed: 16529745]

12. Baudier J, Cole RD. Phosphorylation of Tau-Proteins to A State Like That in Alzheimers Brain Is Catalyzed by A Calcium Calmodulin-Dependent Kinase and Modulated by Phospholipids. J Biol Chem 1987;262:17577–83. [PubMed: 3121601]

13. Bramblett GT, Goedert M, Jakes R, Merrick SE, Trojanowski JQ, Lee VMY. Abnormal tau-phosphorylation at Ser(396) in Alzheimers-disease recapitulates development and contributes to reduced microtubule-binding. Neuron 1993;10:1089–99. [PubMed: 8318230]

14. Alonso AD, Zaidi T, GrundkeIqbal I, Iqbal K. Role of Abnormally Phosphorylated Tan in the Breakdown of Microtubules in Alzheimer-Disease. Proc Natl Acad Sci U S A 1994;91:5562–6. [PubMed: 8202528]

15. Merrick SE, Trojanowski JQ, Lee VMY. Selective destruction of stable microtubules and axons by inhibitors of protein serine/threonine phosphatases in cultured human neurons (NT2N cells). J Neurosci 1997;17:5726–37. [PubMed: 9221771]

16. Wagner U, Utton M, Gallo JM, Miller CCJ. Cellular phosphorylation of tau by GSK-3 beta influences tau binding to microtubules and microtubule organisation. J Cell Sci 1996;109:1537–43. [PubMed: 8799840]

17. Alonso AD, GrundkeIqbal I, Iqbal K. Alzheimer's disease hyperphosphorylated tau sequesters normal tau into tangles of filaments and disassembles microtubules. Nat Med 1996;2:783–7. [PubMed: 8673924]

18. Necula M, Kuret J. Pseudophosphorylation and glycation of tau protein enhance but do not trigger fibrillization in vitro. J Biol Chem 2004;279:49694–703. [PubMed: 15364924]

19. Ishihara T, Hong M, Zhang B, Nakagawa Y, Lee MK, Trojanowski JQ, et al. Age-dependent emergence and progression of a tauopathy in transgenic mice overexpressing the shortest human tau isoform. Neuron 1999;24:751–62. [PubMed: 10595524]

20. Zhang B, Maiti A, Shively S, Lakhani F, McDonald-Jones G, Bruce J, et al. Microtubule-binding drugs offset tau sequestration by stabilizing microtubules and reversing fast axonal transport deficits in a tauopathy model. Proc Natl Acad Sci U S A 2005;102:227–31. [PubMed: 15615853]

21. Sparreboom A, vanAsperen J, Mayer U, Schinkel AH, Smit JW, Meijer DKF, et al. Limited oral bioavailability and active epithelial excretion of paclitaxel (Taxol) caused by P-glycoprotein in the intestine. Proc Natl Acad Sci U S A 1997;94:2031–5. [PubMed: 9050899]

22. Fellner S, Bauer B, Miller DS, Schaffrik M, Fankhanel M, Spruss T, et al. Transport of paclitaxel (Taxol) across the blood-brain barrier in vitro and in vivo. J Clin Invest 2002;110:1309–18. [PubMed: 12417570]

23. Ojima I, Chen J, Sun L, Borella CP, Wang T, Miller ML, et al. Design, synthesis, and biological evaluation of new-generation taxoids. J Med Chem 2008;51:3203–21. [PubMed: 18465846]

24. Ojima I, Slater JC, Michaud E, Kuduk SD, Bounaud PY, Vrignaud P, et al. Syntheses and structure-activity relationships of the second-generation antitumor taxoids: Exceptional activity against drug-resistant cancer cells. J Med Chem 1996;39:3889–96. [PubMed: 8831755]

25. Ojima I, Slater JC, Kuduk SD, Takeuchi CS, Gimi RH, Sun CM, et al. Syntheses and structure-activity relationships of taxoids derived from 14 beta-hydroxy-10-deacetylbaccatin III. J Med Chem 1997;40:267–78. [PubMed: 9022793]

26. Ferlini C, Distefano M, Pignatelli F, Lin S, Riva A, Bombardelli E, et al. Antitumour activity of novel taxanes that act at the same time as cytotoxic agents and P-glycoprotein inhibitors. Br J Cancer 2000;83:1762–8. [PubMed: 11104578]

27. Vredenburg MR, Ojima I, Veith J, Pera P, Kee K, Cabral F, et al. Effects of orally active taxanes on P-glycoprotein modulation and colon and breast carcinoma drug resistance. J Natl Cancer Inst 2001;93:1234–45. [PubMed: 11504769]

28. Cisternino S, Bourasset F, Archimbaud Y, Semiond D, Sanderink G, Scherrmann JM. Nonlinear accumulation in the brain of the new taxoid TXD258 following saturation of P-glycoprotein at the blood-brain barrier in mice and rats. Br J Pharmacol 2003;138:1367–75. [PubMed: 12711638]

29. Metzger-Filho O, Moulin C, de Azambuja E, Ahmad A. Larotaxel: broadening the road with new taxanes. Expert Opin Investig Drugs 2009;18:1183–9.

30. Ballatore C, Hyde E, Deiches RF, Lee VMY, Trojanowski JQ, Huryn D, et al. Paclitaxel C-10 carbamates: Potential candidates for the treatment of neurodegenerative tauopathies. Bioorg Med Chem Lett 2007;17:3642–6. [PubMed: 17485207]

31. Rice A, Liu YB, Michaelis ML, Himes RH, Georg GI, Audus KL. Chemical modification of paclitaxel (Taxol) reduces P-glycoprotein interactions and increases permeation across the blood-brain barrier in vitro and in situ. J Med Chem 2005;48:832–8. [PubMed: 15689167]

32. Lee VMY, Otvos L, Schmidt ML, Trojanowski JQ. Alzheimer-Disease Tangles Share Immunological Similarities with Multiphosphorylation Repeats in the 2 Large Neurofilament Proteins. Proc Natl Acad Sci U S A 1988;85:7384–8. [PubMed: 2459703]

33. Lee CB, Wu ZC, Zhang F, Chappell MD, Stachel SJ, Chou TC, et al. Insights into long-range structural effects on the stereochemistry of aldol condensations: A practical total synthesis of desoxyepothilone F. J Am Chem Soc 2001;123:5249–59. [PubMed: 11457387]

34. Rivkin A, Yoshimura F, Gabarda AE, Chou TC, Dong HJ, Tong WP, et al. Complex target-oriented total synthesis in the drug discovery process: The discovery of a highly promising family of second generation epothilones. J Am Chem Soc 2003;125:2899–901. [PubMed: 12617656]

35. Rivkin A, Yoshimura F, Gabarda AE, Cho YS, Chou TC, Dong HJ, et al. Discovery of (E)-9,10-dehydroepothilones through chemical synthesis: On the emergence of 26-trifluoro-(E)-9,10-dehydro-12,13-desoxyepothilone B as a promising anticancer drug candidate. J Am Chem Soc 2004;126:10913–22. [PubMed: 15339176]

36. Chou TT, Trojanowski JQ, Lee VMY. p38 mitogen-activated protein kinase-independent induction of gadd45 expression in nerve growth factor-induced apoptosis in medulloblastomas. J Biol Chem 2001;276:41120–7. [PubMed: 11544251]

37. Wang Q, Rager JD, Weinstein K, Kardos PS, Dobson GL, Li JB, et al. Evaluation of the MDR-MDCK cell line as a permeability screen for the blood-brain barrier. Int J Pharm 2005;288:349–59. [PubMed: 15620875]

38. Cecchelli R, Berezowski V, Lundquist S, Culot M, Renftel M, Dehouck MP, et al. Modelling of the blood-brain barrier in drug discovery and development. Nat Rev Drug Discov 2007;6:650–61. [PubMed: 17667956]

39. Reichel A. The role of blood-brain barrier studies in the pharmaceutical industry. Curr Drug Metab 2006;7:183–203. [PubMed: 16472107]

40. Summerfield SG, Read K, Begley DJ, Obradovic T, Hidalgo IJ, Coggon S, et al. Central nervous system drug disposition: The relationship between in situ brain permeability and brain free fraction. J Pharmacol Exp Ther 2007;322:205–13. [PubMed: 17405866]
41. Friden M, Gupta A, Antonsson M, Bredberg U, Hammarlund-Udenaes M. In vitro methods for estimating unbound drug concentrations in the brain interstitial and intracellular fluids. Drug Metab Dispos 2007;35:1711–9. [PubMed: 17591680]
42. Altmann KH. Recent developments in the chemical biology of epothilones. Curr Pharm Des 2005;11:1595–613. [PubMed: 15892665]
43. Trojanowski JQ, Smith AB, Huryn D, Lee VMY. Microtubule-stabilising drugs for therapy of Alzheimer's disease and other neurodegenerative disorders with axonal transport impairments. Expert Opin Pharmacother 2005;6:683–6. [PubMed: 15934894]
44. Bollag DM, Mcqueney PA, Zhu J, Hensens O, Koupal L, Liesch J, et al. Epothilones, A New Class of Microtubule-Stabilizing Agents with A Taxol-Like Mechanism of Action. Cancer Res 1995;55:2325–33. [PubMed: 7757983]
45. Andrieux A, Salin P, Schweitzer A, Begou M, Pachoud B, Brun P, et al. Microtubule stabilizer ameliorates synaptic function and behavior in a mouse model for schizophrenia. Biol Psychiatry 2006;60:1224–30. [PubMed: 16806091]
46. O'Reilly T, Wartmann M, Brueggen J, Allegrini PR, Floersheimer A, Maira M, et al. Pharmacokinetic profile of the microtubule stabilizer patupilone in tumor-bearing rodents and comparison of anti-cancer activity with other MTS in vitro and in vivo. Cancer Chemother Pharmacol 2008;62:1045–54. [PubMed: 18301895]
47. Laferriere NB, Macrae TH, Brown DL. Tubulin synthesis and assembly in differentiating neurons. Biochem Cell Biol 1997;75:103–17. [PubMed: 9250358]
48. Black MM, Baas PW, Humphries S. Dynamics of Alpha-Tubulin Deacetylation in Intact Neurons. J Neurosci 1989;9:358–68. [PubMed: 2563279]
49. Zhang Y, Kwon S, Yamaguchi T, Cubizolles F, Rousseaux S, Kneissel M, et al. Mice lacking histone deacetylase 6 have hyperacetylated tubulin but are viable and develop normally. Mol Cell Biol 2008;28:1688–701. [PubMed: 18180281]
50. Beer TM, Higano CS, Saleh M, Dreicer R, Hudes G, Picus J, et al. Phase II study of KOS-862 in patients with metastatic androgen independent prostate cancer previously treated with docetaxel. Invest New Drugs 2007;25:565–70. [PubMed: 17618407]
51. Denduluri N, Low JA, Lee JJ, Berman AW, Walshe JM, Vatas U, et al. Phase II trial of ixabepilone, an epothilone B analog, in patients with metastatic breast cancer previously untreated with taxanes. J Clin Oncol 2007;25:3421–7. [PubMed: 17606971]
52. Cleveland DW, Lopata MA, Sherline P, Kirschner MW. Unpolymerized Tubulin Modulates the Level of Tubulin Messenger-Rnas. Cell 1981;25:537–46. [PubMed: 6116546]
53. Bedard PL, Di Leo A, Piccart-Gebhart MJ. Taxanes: optimizing adjuvant chemotherapy for early-stage breast cancer. Nat Rev Clin Oncol 2010;7:22–36. [PubMed: 19997076]
54. Yoshiyama Y, Higuchi M, Zhang B, Huang SM, Iwata N, Saido TC, et al. Synapse loss and microglial activation precede tangles in a P301S tauopathy mouse model. Neuron 2007;53:337–51. [PubMed: 17270732]
55. Brunden KR, Zhang B, Carroll J, Yao Y, Potuzak JS, Hogan A-ML, et al. Epothilone D improves microtubule densitiry, axonal integrity and cognition in a transgenic mouse model of tauopathy. J Neurosci 2010;30:13861–6. [PubMed: 20943926]

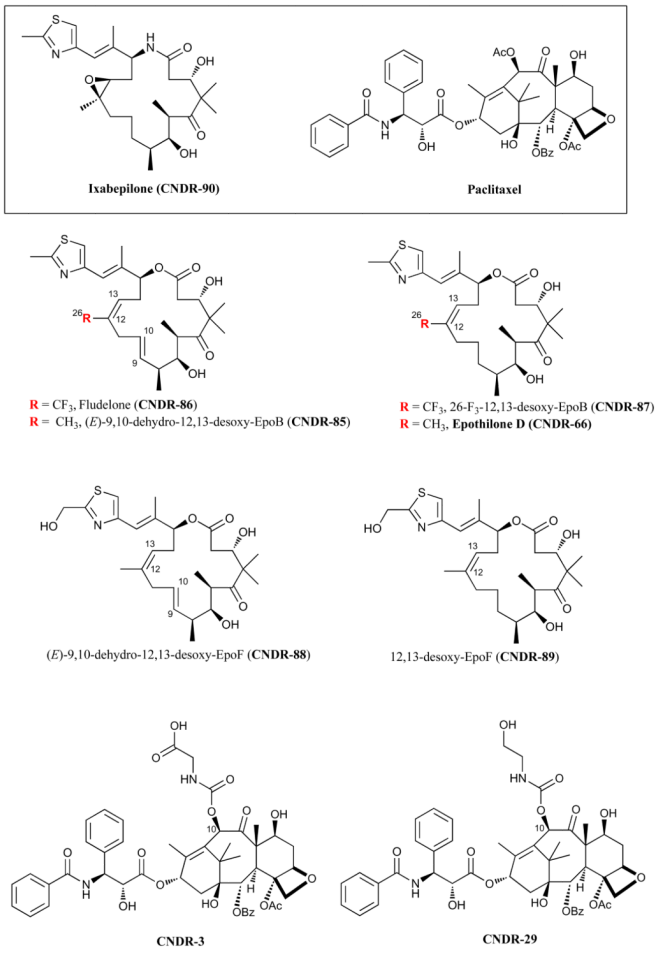

Figure 1.

The structures of evaluated taxanes and epothilones, with their common name and corresponding compound designation used throughout the manuscript.

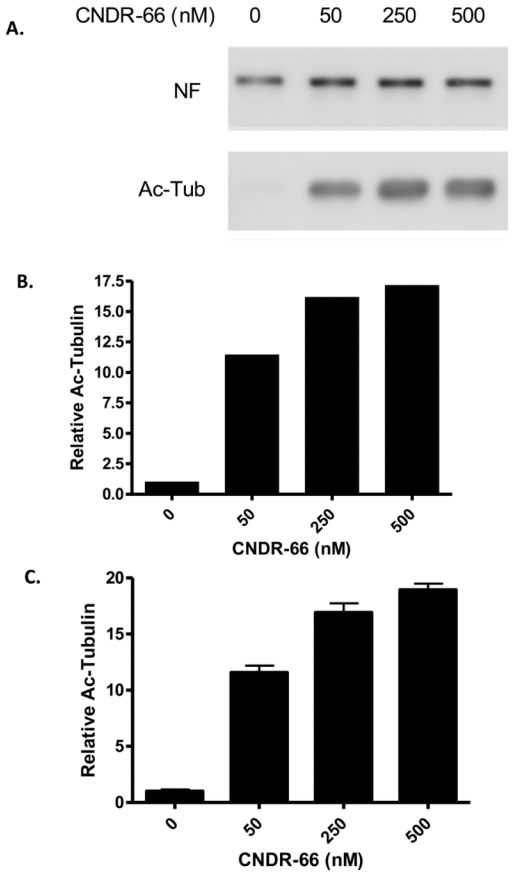

Figure 2.

Validation of the acetyl-tubulin ELISA. PC12 cell cultures were treated for 24 hours with various doses of CNDR-66 and (**A**) aliquots of the cell homogenates were analyzed by SDS-PAGE followed by immunoblotting, with detection of acetyl-tubulin (Ac-Tub) and neurofilament medium chain (NF). The immunoblot underwent densitometric analysis, with acetyl-tubulin values normalized to the corresponding NF values for each treatment condition. These normalized values were then compared to that obtained for the vehicle-treated cultures to obtain relative acetyl-tubulin levels **(B)**. Additional aliquots of the PC12 cell homogenates were used in the acetyl-tubulin ELISA. ELISA values obtained from cell homogenates after CNDR-66 treatment were normalized to the corresponding values from vehicle-treated cultures to obtain relative acetyl-tubulin values **(C)**. Error bars = SEM.

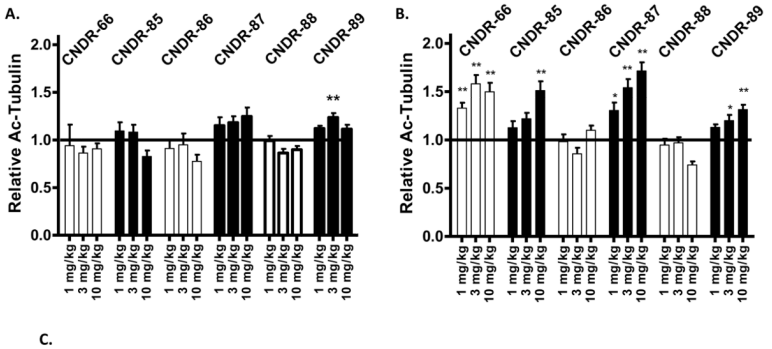

C.

Compd	1 mg/kg				3 mg/kg				10 mg/kg			
	Plasma		Brain		Plasma		Brain		Plasma		Brain	
	ng/ml	nM	ng/g	nM	ng/ml	nM	ng/g	nM	ng/ml	nM	ng/g	nM
CNDR-66	BLD	---	19+/-10	39	BLD	---	50+/-9.1	102	BLD	---	202+/-63	411
CNDR-85	1.9+/-0.3	3.9	20+/-1.0	41	1.7+/-0.4	3.5	61+/-4.2	124	3.7+/-0.7	7.6	189+/-22	386
CNDR-86	BLD	---	8.8+/-4.2	16	0.5+/-0.4	0.9	43+/-4.3	79	BLD	---	160+/-21	294
CNDR-87	BLD	---	6.3+/-1.7	12	BLD	---	20+/-1.2	37	BLD	---	70+/-12	128
CNDR-88	2.8+/-1.0	5.5	2.0+/-1.2	4.0	6.1+/-2.9	12	19+/-5.5	38	8.3+/-4.0	16	66+/-4.4	130
CNDR-89	0.2+/-0.3	0.4	0.8+/-0.9	1.6	BLD	---	4.7+/-0.2	9.3	0.2+/-0.3	0.4	25+/-7.0	49

Figure 3.

Evaluation of epothilone effects on brain and ON acetyl-tubulin levels 16 hours after administration. Mice (n=3/treatment) received a single i.p. administration of epothilones (denoted in the graphs) at doses of 1, 3 or 10 mg/kg, and brain and ON homogenates were prepared for analysis of acetyl-tubulin levels by ELISA. **(A)** Average brain acetyl-tubulin levels after treatment with the various epothilones at multiple doses, with all values normalized to vehicle-treated mice. **(B)** Average ON acetyl-tubulin levels after treatment with epothilones at multiple doses, with all values normalized to vehicle-treated mice. **(C)** Concentrations of the epothilones in plasma and brain 16 hours after drug administration. In A. and B., error bars represent SEM. * $p < 0.05$, ** $p < 0.01$.

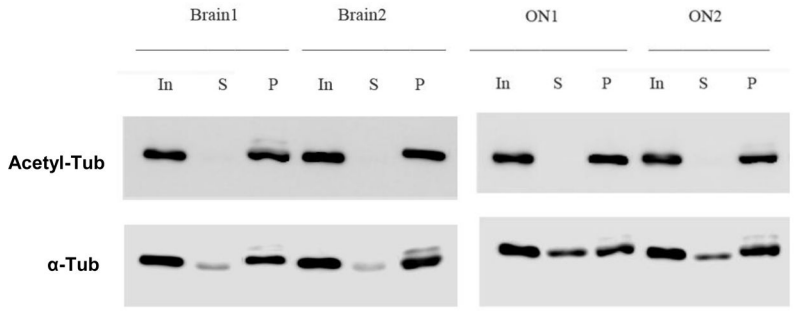

Figure 4.

Evaluation of relative acetylated and deactylated α-tubulin levels in mouse brain and ON. Homogenates from brain and ON (In=input) from mice were immunoprecipitated with acetyl-tubulin antibody. Equal proportions of the unbound supernatant fraction (S) and the material obtained after detergent disruption of immune complexes in the immunoprecipitated pellet (P) were analyzed by SDS-PAGE, followed by immunoblotting with acetyl-tubulin (Acetyl-Tub) or α-tubulin (α-Tub) antibodies. Because acetylated tubulin is quantitatively immunoprecipitated, the amount of α-tubulin within the supernatant (S) fraction represents deacetylated α-tubulin.

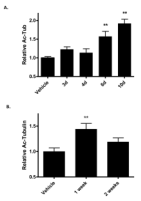

Figure 5.

Time-dependent changes in brain acetyl-tubulin levels in mice treated with CNDR-66. **(A)** Groups of mice received a single administration of 3 mg/kg of CNDR-66 (n=3–6) or vehicle (n=8), and brain homogenates were prepared at various times after treatment for analysis of acetyl-tubulin levels by ELISA. Vehicle-treated data were from homogenates prepared 4 days after vehicle treatment. Average brain acetyl-tubulin levels after CNDR-66 treatment were normalized to vehicle-treated mice. **(B)** Groups of mice (n=3) were administered 3 mg/kg of CNDR-66 or vehicle and brain homogenates were prepared 7 and 14 days after treatment for analysis in the acetyl-tubulin ELISA. Vehicle-treated data were from homogenates prepared 7 days after treatment. Average brain acetyl-tubulin levels after CNDR-66 treatment were normalized to vehicle-treated mice. Error bars for both graphs represent SEM. ** $p < 0.01$.

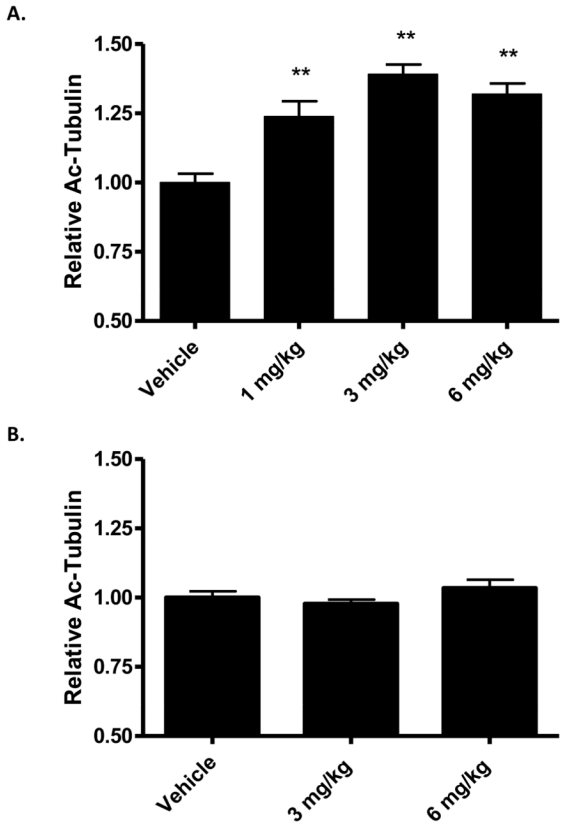

Figure 6.

Dose-dependent effects of CNDR-66 and CNDR-87 on brain acetyl-tubulin levels. Groups of mice (n=3) received a single administration of 1 mg/kg, 3 mg/kg or 6 mg/kg of **(A)** CNDR-66 or **(B)** CNDR-87, and brain homogenates were assessed for acetyl-tubulin levels 7 days after dosing. Average brain acetyl-tubulin levels after drug treatment were normalized to vehicle-treated mice. Error bars for both graphs represent SEM. ** $p<0.01$.

Table 1

Plasma and brain drug levels 2 and 24 hours after i.p. administration of selected taxanes and epothilones.

Compound	2 hours (5 mg/kg)					24 hours (10 mg/kg)				
	Plasma		Brain		B/P[1]	Plasma		Brain		B/P
	ng/ml	SD	ng/g	SD		ng/ml	SD	ng/g	SD	
Paclitaxel	1286	341	85	56	0.07					
CNDR-3	15	3	BLD[2]	--	NC[3]					
CNDR-29	389	109	BLD	--	NC					
CNDR-66	14	4	109	21	7.6	BLD	--	64	11	NC
CNDR-85	5	2	236	21	52.9	1.7	0.4	259	26	157
CNDR-86	20	4	86	21	4.3	0.5	0.4	88	19	118
CNDR-87	1.4	0.6	71	18	52	BLD	--	28	1.9	NC
CNDR-88	12	5	30	10	2.6	6.1	2.9	45	19	7.3
CNDR-89	6.8	1.9	24	10	3.5	BLD	--	13	0.5	NC
CNDR-90	319	110	142	1.4	0.4	41	16	107	24	2.6

[1] B/P = Brain-to-Plasma ratio;

[2] BLD = Below Limit of Detection;

[3] NC = Not Calculated

Table 2

Evaluation of epothilone MT stabilizers for predicted membrane permeability and efflux ratios in MDCK-MDR cells.

Compound	Papp (A-B) (10^{-6} cm/s)	Papp (B-A) (10^{-6} cm/s)	Efflux Ratio (B-A)/(A-B)
CNDR-66	30	46.8	1.6
CNDR-85	8.2	49.8	6.1
CNDR-86	4.4	62.0	14
CNDR-87	11.9	54.8	4.6
CNDR-88	0.8	58.6	73
CNDR-89	2.3	63	28

Table 3

Evaluation of epothilone MT stabilizers for their ability to inhibit Pgp-mediated transport of digoxin.

Compounds	Papp (A-B) (10^{-6} cm/s)	Papp (B-A) (10^{-6} cm/s)	Efflux Ratio (B-A)/(A-B)
1 Digoxin	0.11	4.12	37
1 Digoxin + CNDR-66	0.21	0.29	1.4
2 Digoxin	0.19	8.38	43
2 Digoxin + CNDR-85	0.40	5.95	15
2 Digoxin + CNDR-86	0.32	7.61	24
2 Digoxin + CNDR-87	0.64	4.60	7.2
2 Digoxin + CNDR-88	0.38	6.74	18
2 Digoxin + CNDR-89	0.43	7.72	18

1and 2 denote independent studies.